第51卷第1期 中国科学技术大学学报 Vol. 51, No. 1
2021年1月 JOURNAL OF UNIVERSITY OF SCIENCE AND TECHNOLOGY OF CHINA Jan. 2021
Received: 2021-01-08; Revised: 2021-01-31 doi:10.52396/JUST-2020-0033

Event-triggered sliding mode load frequency control for multi-area interconnected power systems under deception attacks

LIU Xinghua[1*], BAI Dandan[1], SUN Baoren[2], WEN Jiayan[3], LV Wenjun[4], LI Kun[5]
1. School of Electrical Engineering, Xi'an University of Technology, Xi'an 710054, China;
2. Huaneng Chaohu Power Generation Co. LTD, Chaohu 238000, China;
3. School of Electrical and Information Engineering, Guangxi University of Science and Technology, Liuzhou 545616, China;
4. School of Information Science and Technology, University of Science and Technology of China, Hefei 230026, China;
5. Institute of Advanced Technology, University of Science and Technology of China, Hefei 230088, China
* Corresponding author. E-mail: liuxh@xaut.edu.cn

Abstract: In this paper, the problem of sliding mode load frequency control (LFC) is probed for the multi-area interconnected power system under deception attacks. In the case of deception attacks, a Luenberger observer is designed to generate state estimation of the multi-area power systems. An event-triggered mechanism is introduced to reduce the frequency of controller updates and communication between nodes. Sufficient conditions are proposed to achieve asymptotical stability by utilizing sliding mode control and Lyapunov-Krasovskii (L-K) functional method. Then the sliding mode controller is synthesized to ensure that the trajectory of the closed-loop system can be driven onto the prescribed sliding surface. Finally, the effectiveness of the design scheme is verified by a three-area interconnected power system.

Keywords: Load frequency control, deception attacks, sliding mode control, event-triggering mechanism
CLC number: TU459 **Document code**: A

1 Introduction

Small changes in frequency will have serious impact on the interconnected power grid. One reason is that it is difficult to estimate the frequency variation caused by a load, and the second is the area exchange on the tie-line power changes, which will bring challenges to the stability of the frequency[1]. Load frequency control (LFC) is an important means to solve the power grid frequency change caused by load variation. Its main function is to ensure the stability of the load frequency of the multi-area interconnection power systems[2]. Frequency stability is an important index of power quality of the power systems[3]. The target of LFC is mainly realized by adjusting the frequency deviation value of the grid and the exchange power value of the tie-line. However, any sudden change of the load may lead to the deviation frequency, which will then seriously affect the stable operation of the systems. Therefore, to ensure the power quality and system stability, an LFC system is required to adjust the frequency of the systems to the rated value and maintain the exchange power of the regional tie-line as the planned value.

In recent years, with the rapid development of computer network and communication technology, an important type of network control systems (NCS) has been formed. On the one hand, these developments can improve the monitoring efficiency of the power systems and promote information communication. On the other hand, this also leads to the possibility of network attacks on the power systems, and brings challenges to the network security. Hence, it is urgent to analyze the network attacks and study the network security under the network attacks[4-10]. The deception attack is an attack approach in which the attackers impersonate a normal user to gain access to the target or obtain key information, which belongs to such attack techniques as obtaining passwords, malicious codes and the network deception. Deception attacks will affect the stability of power systems operation, and cause systems to breakdown in serious cases. In references[4-6], an advanced resilience event-triggered LFC scheme is proposed, which can reduce the communication burden while resisting DoS attacks in terms of the defense effect and the average trigger period. In references[7-9], , the multi-area LFC power systems under hybrid network attacks, including DoS attacks and deception attacks are

Citation: LIU Xinghua, BAI Dandan, SUN Baoren, et al. Event-triggered sliding mode load frequency control for multi-area interconnected power systems under deception attacks. J. Univ. Sci. Tech. China, 2021, 51(1): 33-42.

studied, and a switching system model with DoS attacks and stochastic deception attacks is established. The stabilization problem of the distributed network control systems under stochastic deception attacks is studied and a decentralized mixed sampling-data strategy is proposed in reference [10] by using the hybrid nondirectional triggering mechanism.

In view of the above network attacks, there exist the robust control[11,12], sliding mode control (SMC)[13-15], fuzzy control[16], static feedback output control[17] and other methods. A robust state observer is designed[12], which can be used as a detection monitor with guaranteed performance. In reference [13], the finite time convergence problem of the sliding mode variable structure control is considered for a class of uncertain multivariable linear systems, where an exponential nonlinear convergent sliding hypersurface is proposed and its corresponding control scheme is provided. Huang et al[14] establish an adaptive integral sliding-mode control for cyber-physical systems against a class of actuator attacks. Tang et al[15] propose a position sliding mode control for DC-motor position tracking based on a high-gain observer. Compared with other control strategies, the sliding mode control can be independent of object parameters and has no need of online system identification, which shows insensitivity to parameter changes and disturbances.

To sum up, this paper studies the LFC problem of the multi-area interconnected power systems under deception attacks. So far, this paper is the first to use the event-triggered sliding mode control to solve such problems. The main contributions of this paper are described below.

(Ⅰ) The event-triggered sliding mode LFC under deception attacks is modeled, which lays a foundation for studying the security of multi-area interconnected power systems.

(Ⅱ) Aiming at the security problem of the multi-area interconnected power systems, the event-triggered sliding mode LFC strategy is proposed in this paper to realize the stable operation of the systems under deception attacks, which can avoid a lot of unnecessary data transmission and effectively save network resources.

(Ⅲ) The simulated results of a three-area interconnected power system in a simulation case show the effectiveness of the proposed strategy.

The rest of this paper is organized as follows. In Section 2, we present the dynamic model of the event-triggered sliding mode LFC under deception attacks. In Section 3, we analyze the stability of the system and carries on the accessibility analysis. A simulation case is used to verify the proposed method in Section 4. Finally, Section 5 concludes this paper.

Notations The following notations are used throughout this paper. $\mathbb{E}\{\cdot\}$ represents mathematical expectations. $\mathrm{diag}\{\cdot\}$ represents the diagonal matrix. Let $\|x\|$ and $\|A\|$ be the Euclidean norm of a vector x and a matrix A, respectively. For a symmetric block matrix, we use $*$ to denote the terms introduced by symmetry. We use $\mathbb{R}^n$ to denote the n-dimensional Euclidean space. $\mathrm{sym}(A)$ represents $A+A^{\mathrm{T}}$.

2 System description and preliminaries

The system model

Firstly, the dynamic model of multi-area power systems is described as follows[8]

$$\left.\begin{aligned}\dot{x}(t) &= Ax(t) + Bu(t) + F\omega(t)\\ y(t) &= Cx(t)\end{aligned}\right\} \tag{1}$$

where $x(t) = [x_1^{\mathrm{T}}(t), x_2^{\mathrm{T}}(t), \cdots, x_N^{\mathrm{T}}(t)]^{\mathrm{T}}$, $y(t) = [y_1^{\mathrm{T}}(t), y_2^{\mathrm{T}}(t), \cdots, y_N^{\mathrm{T}}(t)]^{\mathrm{T}}$, $u(t) = [u_1^{\mathrm{T}}(t), u_2^{\mathrm{T}}(t), \cdots, u_N^{\mathrm{T}}(t)]^{\mathrm{T}}$, $\omega(t) = [\omega_1^{\mathrm{T}}(t), \omega_2^{\mathrm{T}}(t), \cdots, \omega_N^{\mathrm{T}}(t)]^{\mathrm{T}}$, $x_i(t) = [\Delta f_i, \Delta P_{mi}, \Delta P_{vi}, \int_0^t \mathrm{ACE}_i(s)\mathrm{d}s, \Delta P_{tie-i}]^{\mathrm{T}}$, $y_i(t) = [\mathrm{ACE}_i, \int_0^t \mathrm{ACE}_i(s)\mathrm{d}s]^{\mathrm{T}}$, $\omega_i(t) = \Delta\{P_d\}_i(t)$ and

$$B = \mathrm{diag}[B_1, \cdots, B_N], C = \mathrm{diag}[C_1, \cdots, C_N],$$

$$F = \mathrm{diag}[F_1, \cdots, F_N], B_i = \begin{bmatrix} 0 & 0 & \dfrac{1}{T_{gi}} & 0 & 0 \end{bmatrix}^{\mathrm{T}},$$

$$C_i = \begin{bmatrix} \beta_i & 0 & 0 & 0 & 1 \\ 0 & 0 & 0 & 1 & 0 \end{bmatrix}^{\mathrm{T}},$$

$$F_i = \begin{bmatrix} -\dfrac{1}{M_i} & 0 & 0 & 0 & 0 \end{bmatrix}^{\mathrm{T}}, A = [A_{ij}]_{N\times N},$$

$$A_{ij} = \begin{bmatrix} 0 & 0 & 0 & 0 & 0 \\ 0 & 0 & 0 & 0 & 0 \\ 0 & 0 & 0 & 0 & 0 \\ 0 & 0 & 0 & 0 & 0 \\ -2\pi T_{ij} & 0 & 0 & 0 & 0 \end{bmatrix}, T_{ij} = T_{ji},$$

$$A_{ii} = \begin{bmatrix} \dfrac{D_i}{M_i} & \dfrac{1}{M_i} & 0 & 0 & -\dfrac{1}{M_i} \\ 0 & -\dfrac{1}{T_{chi}} & \dfrac{1}{T_{chi}} & 0 & 0 \\ -\dfrac{1}{\widehat{R}_i T_{gi}} & 0 & -\dfrac{1}{T_{gi}} & 0 & 0 \\ \beta_i & 0 & 0 & 0 & 1 \\ 2\pi \sum\limits_{j=1, j\neq i}^{N} T_{ij} & 0 & 0 & 0 & 0 \end{bmatrix}.$$

The state variables Δf_i, ΔP_{tie-}, ΔP_{mi}, ΔP_{vi}, and ΔP_{di} are the systems frequency deviation value, tie-line power deviation value, mechanical power deviation value, regulator position value and load of the i subregion, respectively. R_i, M_i, D_i, T_{chi} and T_{gi} are the velocity sag coefficient, the generator moment of inertia, the generator damping coefficient, the steam capacity time constant and the governor time constant,

respectively. β_i is the conversion factor between systems power and frequency. It should be noted that the area control error (ACE) of each region i is not only related to the frequency deviation, but also related to the power exchange of the tie-line between regions, which is defined as follows

$$\mathrm{ACE}_i = \beta_i \Delta f_i + \Delta P_{tie-i}.$$

We also consider deception attacks, which completely replace the transmitted data with malicious attack signals, thus destroying the transmission of data. This paper assumes that deception attacks occurred randomly, by the statistical property with the given Bernoulli random variable $\alpha(t) \in \{0,1\}$ in guarantee, the expectation of $E\alpha(t) = \alpha_0$. We can derive the damage measurement value as

$$\bar{y}(t) = y(t) + \alpha(t)\nu(t),$$

where $\nu(t) = -y(t) + \zeta(t)$ for the deception attack signals sent by the attacker, $\zeta(t)$ is an energy constrained signal belonging to $L_2[0,\infty]$. $\alpha(t)$ is a stochastic variable conforming to Bernoulli distribution

$$\mathrm{Prob}\{\alpha(t) = 1\} = E\alpha(t) := \alpha_0;$$
$$\mathrm{Prob}\{\alpha(t) = 0\} = 1 - E\alpha(t) := 1 - \alpha_0;$$

where $\alpha_0 \in [0,1]$ represents the probability of deception attacks. Therefore, after the systems is attacked by deception attacks, the model was rewritten as

$$\left.\begin{aligned} \dot{x}(t) &= Ax(t) + Bu(t) + F\omega(t) \\ y(t) &= (1-\alpha(t))Cx(t) + \alpha(t)\zeta(t) \end{aligned}\right\} \quad (2)$$

It is worth noting that the Bernoulli stochastic variable $\alpha(t)$ can characterize the stochastic occurrence of deception attacks. More specifically, if $\alpha(t)=1$, the output $y(t)=\alpha(t)\zeta(t)$, which means that deception attacks occurs during transmission. If $\alpha(t)=0$, the output $y(t)=Cx(t)$, indicating that the sampling measurement was successfully transmitted to the sliding mode controller.

2.2 The event-triggered the sliding mode load frequency control

Generally, NCS adopts a periodic control strategy, which refers to sampling at equal intervals at discrete time points. At two adjacent time points, the control signal remains unchanged due to the effect of zero-order hold (ZOH). The periodic sampling control is easy to be realized by using existing sampling theorems, but it also has many disadvantages. For example, a large number of useless sampled data will be generated, which will increase the network transmission load and occupy the network communication resources. The event-triggered mechanism can decide whether to transmit data according to judgment rules, which can effectively save the occupation of network resources, reduce the power consumption of network nodes, and thus increasing the service life of network nodes. The basic idea of its design is that, on the premise of ensuring that the systems meets the performance conditions, when the transmitted system signal meets the conditions set in the event generator, the signal is successfully sent once.

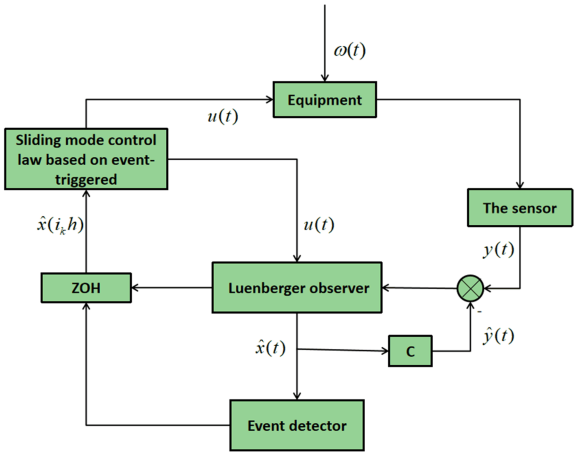

Figure 1. The control system with an event-triggered.

Figure 1 shows the control systems based on the event-triggered. As can be seen from Figure 1, to reduce the amount of data transmission, we added an event detector based on the Luenberger observer in the sliding mode controller channel. The following is the trigger condition of the event-triggered mechanism based on Luenberger observer

$$t_{k+1}h = t_k h + \min_{l\in N} lh \mid e_{\hat{x}}^{\mathrm{T}}(t)\Phi e_{\hat{x}}(t) > \sigma \hat{x}^{\mathrm{T}}(t_k h)\Phi \hat{x}(t_k h) \quad (3)$$

$$e_{\hat{x}}(t) = \hat{x}(i_k h) - \hat{x}(t_k h) \quad (4)$$

where $i_k h = t_k h + lh$, $l \in N$. $i_k h \in (t_k h, t_{k+1} h]$, $t_k (k=0,1,2,\cdots)$, $t_{k+1}h$ and $t_k h$ are respectively the sampling time of two adjacent signals transmitted to the controller that meet the trigger condition, the trigger matrix Φ is a positive definite matrix to be solved, h is the sampling period of LFC, and the event-triggered parameter σ is a preset constant. In simple terms, when trigger condition (3) is met, it will trigger once and data will be updated. Otherwise, it will not trigger.

The Luenberger observer is designed as

$$\left.\begin{aligned} \dot{\hat{x}}(t) &= A\hat{x}(t) + Bu(t) + L[y(t) - \hat{y}(t)] \\ \hat{y}(t) &= (1-\alpha(t))C\hat{x}(t) \end{aligned}\right\} \quad (5)$$

where L is the observer gain, which can be obtained by the linear matrix inequality. $\hat{x}(t)$ is the state estimation vector, $\hat{y}(t)$ is the measured output estimation vector.

Define the systems error as $e(t)=x(t)-\hat{x}(t)$, we have

$$\dot{e}(t) = Ae(t) - L[(1-\alpha(t))Ce(t) + \alpha(t)\zeta(t)] + F\omega(t) \quad (6)$$

According to the observer function, we design the sliding surface as

$$s(t) = B^{\mathrm{T}} X[\hat{x}(t) - \int_0^t (A + BK)\hat{x}(\theta)\mathrm{d}\theta] \quad (7)$$

where K and X are coefficient matrices. Select K to make $A+BK$ satisfy Hurwitz matrix, and the design of X satisfies $B^{\mathrm{T}}XB$ is a non-singular matrix.

Substitute equation (7) into equation (5), we get

$$\begin{aligned}\dot{s}(t) = {} & B^{\mathrm{T}}X\dot{\hat{x}}(t) - B^{\mathrm{T}}X(A+BK)\hat{x}(t) = \\ & B^{\mathrm{T}}XBu(t) - B^{\mathrm{T}}XBK\hat{x}(t) + \\ & B^{\mathrm{T}}XL[(1-\alpha(t))Ce(t) + \alpha(t)\zeta(t)]\end{aligned} \tag{8}$$

Let $\dot{s}(t)=0$, we can get the equivalent input as

$$\begin{aligned}u_{eq}(t) = {} & K\hat{x}(t) - (B^{\mathrm{T}}XB)^{-1}B^{\mathrm{T}} \times \\ & [(1-\alpha(t))Ce(t) + \alpha(t)\zeta(t)]\end{aligned} \tag{9}$$

Define $\eta(t)=t-i_k h$, by using equation (4) and substituting the equivalent input (9) into the observer equation (5), we can obtain the event-triggered SMC dynamic equation as

$$\begin{aligned}\dot{\hat{x}}(t) = {} & A\hat{x}(t) + BK\hat{x}(t-\eta(t)) - BKe_{\hat{x}}(t) + \\ & (L - B(B^{\mathrm{T}}XB)^{-1}B^{\mathrm{T}}XL)[(1-\alpha(t)Ce(t) + \alpha(t)\zeta(t)] = \\ & A\hat{x}(t) + BK\hat{x}(t-\eta(t)) - BKe_{\hat{x}}(t) + \\ & \bar{B}[(1-\alpha(t)Ce(t) + \alpha(t)\zeta(t)],\end{aligned}$$

where $\bar{B}=L-B(B^{\mathrm{T}}XB)^{-1}B^{\mathrm{T}}XL$, $0\leqslant\eta(t)\leqslant\bar{\eta}$, $\bar{\eta}$ is the maximum upper bound of delay, \ *mu* and $\bar{\eta}$ are constants.

From what has been discussed above, the sliding mode LFC model based on sample error is as

$$\left.\begin{aligned}\dot{\hat{x}}(t) = {} & A\hat{x}(t) + BK\hat{x}(t-\eta(t)) - BKe_{\hat{x}}(t) + \\ & \bar{B}[(1-\alpha(t)Ce(t) + \alpha(t)\zeta(t)] \\ \dot{e}(t) = {} & Ae(t) - L[(1-\alpha(t))Ce(t) + \\ & \alpha(t)\zeta(t)] + F\omega(t)\end{aligned}\right\} \tag{10}$$

For the convenience of later calculation, the formula (10) is divided into the following two parts.

$$\left.\begin{aligned}\dot{e}(t) = {} & \varphi(t) + (\alpha_0 - \alpha(t))\psi(t) \\ \varphi(t) = {} & Ae(t) - L[(1-\alpha_0)Ce(t) + \\ & \alpha_0\zeta(t)] + F\omega(t) \\ \psi(t) = {} & -LCe(t) + L\zeta(t)\end{aligned}\right\} \tag{11}$$

$$\left.\begin{aligned}\dot{\hat{x}}(t) = {} & \Delta(t) + (\alpha_0 - \alpha(t))\Omega(t), \\ \Delta(t) = {} & A\hat{x}(t) + BK\hat{x}(t-\eta(t)) - BKe_{\hat{x}}(t) + \\ & \bar{B}[(1-\alpha_0)Ce(t) + \alpha_0\zeta(t)] \\ \Omega(t) = {} & \bar{B}Ce(t) - \bar{B}\zeta(t)\end{aligned}\right\} \tag{12}$$

Definition 2.1 The main purpose of this paper is to analyze the stability of multi-area LFC systems under deception attacks, and design the sliding mode controller. When the following conditions are met, the closed-loop system (10) are asymptotically stable, and the disturbance suppression level of H_∞ is γ.

(Ⅰ) When $\omega(t)=0$ and $\zeta(t)=0$, the system (10) are asymptotically stable;

(Ⅱ) Under zero initial conditions, for any non-zero $\omega(t)\in L_2[0,\infty]$ and $\zeta(t)\in L_2[0,\infty]$, if the following inequality is true, then the multi-area power system (10) satisfy the performance of H_∞ and the disturbance suppression level is γ.

$$\mathrm{E}\{\|\hat{y}(t)\|_2\} \leqslant \gamma\mathrm{E}\{\|\omega(t)\|_2 + \|\zeta(t)\|_2\}.$$

Lemma 2.1[18] For any real vector u, v and a symmetric positive matrix Q with compatible dimensions, the following inequality is true.

$$u^{\mathrm{T}}v + v^{\mathrm{T}}u \leqslant u^{\mathrm{T}}Qu + v^{\mathrm{T}}Q^{-1}v.$$

Lemma 2.2[19] Schur Complement Lemma For given constant matrices S_{11}, S_{12}, S_{22} with appropriate dimensions and $S=\begin{bmatrix}S_{11} & S_{12}\\ S_{12}^{\mathrm{T}} & S_{22}\end{bmatrix}<0$, then the following two conditions are equivalent.

(i) $S_{11}<0$, $S_{22}-S_{12}^{\mathrm{T}}S_{11}^{-1}S_{12}<0$;

(ii) $S_{22}<0$, $S_{11}-S_{12}^{\mathrm{T}}S_{22}^{-1}S_{12}<0$.

3 Main results

By introducing the lemma and mathematical derivation above, we first give the stability analysis of H_∞ of the sliding mode load frequency control model of multi-area interconnection power systems under deception attacks, and give the sufficient condition of the asymptotic stability as shown in Theorem 3.1 and Theorem 3.2. The reachability analysis is then given in Theorem 3.3.

3.1 System stability analysis

Theorem 3.1 For given level of disturbance rejection $\gamma>0$, scalar $\alpha_0\geqslant 0$, the closed-loop system (10) asymptotically stable, and meet the H_∞ performance, if there exist appropriate dimensions of the positive definite matrices Q_1, Q_2, W_1, W_2, L, symmetric positive definite matrix X and matrices U, N with appropriate dimensions to make the following inequality is established.

$$\begin{bmatrix}\Gamma_{11} & \Gamma_{12}\\ \Gamma_{12}^{\mathrm{T}} & \Gamma_{22}\end{bmatrix} < 0 \tag{13}$$

$$\Theta_1 = \begin{bmatrix}Q_2 & U^{\mathrm{T}}\\ U & Q_2\end{bmatrix} > 0,\ \Theta_2 = \begin{bmatrix}W_2 & N^{\mathrm{T}}\\ N & W_2\end{bmatrix} \tag{14}$$

where

$$\Gamma_{11} = \Gamma_{111} - \Gamma_{112} - \Gamma_{113},$$

$$\Gamma_{111} = \begin{bmatrix}Z_1 & Z_2\\ Z_2^{\mathrm{T}} & Z_3\end{bmatrix},$$

$$Z_1 = \begin{bmatrix}\Sigma_1 & \mathrm{XBK} & & (1-\alpha_0)\mathrm{XLC} & 0\\ * & \Sigma_2 & 0 & 0 & 0\\ * & * & 0 & 0 & 0\\ * & * & * & \Sigma_3 & 0\\ * & * & * & * & 0\end{bmatrix},$$

$$Z_2 = \begin{bmatrix}0 & -\mathrm{XBK} & 0 & \alpha_0 XL\\ 0 & \sigma\Phi & 0 & 0\\ 0 & 0 & 0 & 0\\ 0 & 0 & XF & -\alpha_0 XL\\ 0 & 0 & 0 & 0\end{bmatrix},$$

$$Z_3 = \begin{bmatrix} 0 & 0 & 0 & 0 \\ * & (\sigma-1)\Phi & 0 & 0 \\ * & * & -\gamma^2 I & 0 \\ * & * & * & -\gamma^2 I \end{bmatrix},$$

$$\Sigma_1 = \mathrm{sym}\{XA\} + Q_1, \Sigma_2 = \sigma\Phi,$$

$$\Sigma_3 = \mathrm{sym}\{XA\} - (1-\alpha_0)\mathrm{XLC} + W_1,$$

$$\Gamma_{112} = \Pi_1^{\mathrm{T}}\Theta_1\Pi_1 + \Pi_2^{\mathrm{T}}\Theta_2\Pi_2 + Y_1^{\mathrm{T}}Y_1,$$

$$\Pi_1 = [e_1 - e_2 \quad e_2 - e_3]^{\mathrm{T}},$$

$$\Pi_2 = [e_4 - e_5 \quad e_5 - e_6]^{\mathrm{T}},$$

$$Y_1 = [(1-\alpha_0)C \quad 0^{1\times 8}]^{\mathrm{T}},$$

$$\Gamma_{113} = \Xi_1^{\mathrm{T}}\Xi_2^{-1}\Xi_1,$$

$$\Xi_1 = \mathrm{col}[\hat{\eta}Q_2H_\Delta \quad \hat{\eta}Q_2H_\Omega \quad \hat{\eta}W_2H_\varphi \quad \hat{\eta}W_2H_\psi],$$

$$\Xi_2 = \mathrm{diag}\{Q_2, -Q_2, -W_2, -W_2\},$$

$$H_\varphi = [0^{1\times 3} \quad A-(1-\alpha_0)LC \quad 0^{1\times 3} \quad F \quad \alpha_0 L],$$

$$H_\psi = [0^{1\times 3} \quad -LC \quad 0^{1\times 4} \quad L],$$

$$H_\Omega = [0^{1\times 3} \quad \bar{B}C \quad 0^{1\times 4} \quad -\bar{B}],$$

$$H_\Delta = [A \quad BK \quad 0 \quad (1-\alpha_0)\bar{B}C \quad 0 \quad 0 \quad -BK \quad 0 \quad \alpha_0],$$

$$\Gamma_{12} = \begin{bmatrix} XB & 0 & 0 \\ 0^{2\times 1} & 0^{2\times 1} & 0^{2\times 1} \\ 0 & (1-\alpha_0)C^{\mathrm{T}}L^{\mathrm{T}}X & 0 \\ 0^{4\times 1} & 0^{4\times 1} & 0^{4\times 1} \\ 0 & 0 & \alpha_0 L^{\mathrm{T}}X \end{bmatrix},$$

$$\Gamma_{22} = \begin{bmatrix} -B^{\mathrm{T}}XB & 0 & 0 \\ * & -(1-\alpha_0)X & \\ * & * & -\alpha_0 X \end{bmatrix}$$

Proof First, the L-K functional is constructed as

$$V(t) = V_{\hat{x}}(t) + V_e(t),$$

$$V_{\hat{x}}(t) = \hat{x}^{\mathrm{T}}(t)X\hat{x}(t) + \int_{t-\eta(t)}^{t}\hat{x}^{\mathrm{T}}(v)Q_1\hat{x}(v)\mathrm{d}v + \hat{\eta}\int_{t-\hat{\eta}}^{t}\int_{u}^{t}\hat{x}^{\mathrm{T}}(v)Q_2\hat{x}(v)\mathrm{d}u\mathrm{d}v,$$

$$V_e(t) = \{e^{\mathrm{T}}(t)Xe(t) + \int_{t-\eta(t)}^{t}e^{\mathrm{T}}(v)W_1e(v)\mathrm{d}v + \hat{\eta}\int_{t-\hat{\eta}}^{t}\int_{u}^{t}e^{\mathrm{T}}(v)W_2e(v)\mathrm{d}u\mathrm{d}v + e_{\hat{x}}^{\mathrm{T}}(t)\Phi e_{\hat{x}}(t) - e_{\hat{x}}^{\mathrm{T}}(t)\Phi e_{\hat{x}}(t).$$

Then we have

$$E\{\dot{V}(t)\} = E\{\dot{V}_{\hat{x}}(t)\} + E\{\dot{V}_e(t)\},$$

$$E\{\dot{V}_{\hat{x}}(t)\} = 2\hat{x}^{\mathrm{T}}(t)X\Delta + \hat{x}^{\mathrm{T}}Q_1\hat{x} + \Delta^{\mathrm{T}}(t)\hat{\eta}^2 \times Q_2\Delta(t) + \alpha_0(1-\alpha_0)\Omega^{\mathrm{T}}(t)\hat{\eta}^2Q_2\Omega(t) - \hat{\eta}\int_{t-\hat{\eta}}^{t}\dot{\hat{x}}^{\mathrm{T}}(v)Q_2\dot{\hat{x}}(v)\mathrm{d}v =$$

$$2\hat{x}^{\mathrm{T}}(t)XA\hat{x}(t) + 2\hat{x}^{\mathrm{T}}(t)\mathrm{XBK} \times \hat{x}(t-\eta(t)) - 2\hat{x}^{\mathrm{T}}(t)\mathrm{XBK}e_{\hat{x}}(t) + 2(1-\alpha_0)\hat{x}^{\mathrm{T}}(t)X \times LCe(t) - 2(1-\alpha_0)\hat{x}^{\mathrm{T}}(t)XB(B^{\mathrm{T}}XB)^{-1} \times B^{\mathrm{T}}\mathrm{XLC}e(t) + 2\alpha_0\hat{x}^{\mathrm{T}}(t)XL\zeta(t) - 2\alpha_0 \times \hat{x}^{\mathrm{T}}(t)XB(B^{\mathrm{T}}XB)^{-1}B^{\mathrm{T}}XL\zeta(t) + \hat{x}^{\mathrm{T}}(t)Q_1 \times \hat{x}(t) + \Delta^{\mathrm{T}}(t)\hat{\eta}^2Q_2\Delta(t) + \alpha_0(1-\alpha_0)\Omega^{\mathrm{T}}(t) \times \hat{\eta}^2Q_2\Omega(t) - \hat{\eta}\int_{t-\hat{\eta}}^{t}\dot{\hat{x}}^{\mathrm{T}}(v)Q_2\dot{\hat{x}}(v)\mathrm{d}v,$$

$$E\{\dot{V}_e(t)\} = 2e^{\mathrm{T}}(t)X\varphi(t) + e^{\mathrm{T}}(t)W_1e(t) + \varphi^{\mathrm{T}}(t)\hat{\eta}^2W_2\varphi(t) + \alpha_0(1-\alpha_0)\psi^{\mathrm{T}}(t)\hat{\eta}^2W_2\psi(t) - \hat{\eta}\int_{t-\hat{\eta}}^{t}\dot{e}^{\mathrm{T}}(v)W_2\dot{e}(v)\mathrm{d} =$$

$$2e^{\mathrm{T}}(t)XAe(t) - 2(1-\alpha_0)e^{\mathrm{T}}(t)X\,LCe(t) - 2\alpha_0e^{\mathrm{T}}(t)XL\zeta(t) + 2e^{\mathrm{T}}(t)XF\omega(t) + e^{\mathrm{T}}(t)W_1e(t) + \varphi^{\mathrm{T}}(t)\hat{\eta}^2W_2\varphi(t) + \alpha_0(1-\alpha_0)\psi^{\mathrm{T}}(t)\hat{\eta}^2W_2\psi(t) - \hat{\eta}\int_{t-\hat{\eta}}^{t}\dot{e}^{\mathrm{T}}(v)W_2\dot{e}(v)\mathrm{d}v + e_{\hat{x}}^{\mathrm{T}}(t)\Phi e_{\hat{x}}(t) - e_{\hat{x}}^{\mathrm{T}}(t)\Phi e_{\hat{x}}(t).$$

Apply Lemma 2.1 and we get

$$-2(1-\alpha_0)\hat{x}^{\mathrm{T}}(t)XB(B^{\mathrm{T}}XB)^{-1}B^{\mathrm{T}}\mathrm{XLC}e(t) \leqslant (1-\alpha_0)\hat{x}^{\mathrm{T}}(t)XB(B^{\mathrm{T}}XB)^{-1}B^{\mathrm{T}}X\hat{x}(t)B^{\mathrm{T}}X\hat{x}(t) + (1-\alpha_0)e^{\mathrm{T}}(t)C^{\mathrm{T}}L^{\mathrm{T}}\mathrm{XLC}e(t),$$

$$-2\alpha_0x^{\mathrm{T}}(t)XB(B^{\mathrm{T}}XB)^{-1}B^{\mathrm{T}}XL\zeta(t) \leqslant \alpha_0\hat{x}^{\mathrm{T}}(t)XB(B^{\mathrm{T}}XB)^{-1}B^{\mathrm{T}}X\hat{x}(t) + \alpha_0\zeta^{\mathrm{T}}(t)L^{\mathrm{T}}XL\zeta(t).$$

Define

$$(t) = \mathrm{col}[\hat{x}^{\mathrm{T}}(t), \hat{x}^{\mathrm{T}}(t-\eta(t)), \hat{x}^{\mathrm{T}}(t-\hat{\eta}), e^{\mathrm{T}}(t), e^{\mathrm{T}}(t-\eta(t)), e^{\mathrm{T}}(t-\hat{\eta}), e_{\hat{x}}^{\mathrm{T}}(t), \omega^{\mathrm{T}}(t), \zeta^{\mathrm{T}}(t)],$$

By using the inverse convex method in reference [20] to deal with the expected cross terms, we can get

$$-\bar{\eta}\int_{t-\bar{\eta}}^{t}\dot{\hat{x}}^{\mathrm{T}}(v)Q_2\dot{\hat{x}}(v)\mathrm{d}v \leqslant -\begin{bmatrix} \hat{x}(t) - \hat{x}(t-\eta(t)) \\ \hat{x}(t-\eta(t)) - \hat{x}(t-\bar{\eta}) \end{bmatrix}\begin{bmatrix} Q_2 & U^{\mathrm{T}} \\ U & Q_2 \end{bmatrix}\begin{bmatrix} \hat{x}(t) - \hat{x}(t-\eta(t)) \\ \hat{x}(t-\eta(t)) - \hat{x}(t-\bar{\eta}) \end{bmatrix} = -\xi^{\mathrm{T}}(t)\Pi_1^{\mathrm{T}}\Theta_1\Pi_1\xi(t),$$

$$-\bar{\eta}\int_{t-\bar{\eta}}^{t}\dot{e}^{\mathrm{T}}(v)W_2\dot{e}(v)\mathrm{d}v \leqslant -\begin{bmatrix} e(t) - e(t-\eta(t)) \\ e(t-\eta(t)) - e(t-\bar{\eta}) \end{bmatrix}^{\mathrm{T}}\begin{bmatrix} W_2 & N^{\mathrm{T}} \\ N & W_2 \end{bmatrix}\begin{bmatrix} e(t) - e(t-\eta(t)) \\ e(t-\eta(t)) - e(t-\bar{\eta}) \end{bmatrix} = -\xi^{\mathrm{T}}(t)\Pi_1^{\mathrm{T}}\Theta_1\Pi_1\xi(t).$$

Remark 1 In this paper, the inverse convex method in reference [20] and the free weighted matrix method are used to deal with the integral coupling term, which greatly reduce the conservatism of the closed-loop system (10).

According to the proposed event-triggered equations (3) and (4) can be guaranteed

$$e_{\hat{x}}^{\mathrm{T}}(t)\Phi e_{\hat{x}}(t) < \sigma(\hat{x}(t-\eta(t)) - e_{\hat{x}}(t))^{\mathrm{T}}\Phi(\hat{x}(t-\eta(t)) - e_{\hat{x}}(t)).$$

From what has been discussed above, we can conclude that

$$E\{\dot{V}(t)\} + E\hat{y}^{\mathrm{T}}(t)\hat{y}(t) - \gamma^2 E\omega^{\mathrm{T}}(t)\omega(t) + \zeta^{\mathrm{T}}(t)\zeta(t)\} \leqslant \xi^{\mathrm{T}}(t)(\Gamma_{11} - \Gamma_{12}\Gamma_{22}^{-1}\Gamma_{12}^{\mathrm{T}})\xi(t).$$

By using Lemma 2.2 (Schur complement theorem), we can get $\Gamma_{11} - \Gamma_{12}\Gamma_{22}^{-1}\Gamma_{12}^{\mathrm{T}} < 0$ and further derive

$$E\{\dot{V}(t)\} < -E\{\hat{y}^{\mathrm{T}}\}(t)\hat{y}(t)\} + \gamma^2 E\{\omega^{\mathrm{T}}\}(t)\omega(t) + \{\zeta^{\mathrm{T}}\}(t)\zeta(t)\}.$$

Integrate both sides of this equation and we have

$$E\{V(+\infty)\} - E\{V(0)\} < E\int_0^{+\infty}[-\{\hat{y}^{\mathrm{T}}(t)\hat{y}(t)] + \gamma^2[\omega^{\mathrm{T}}(t)\omega(t) + \zeta^{\mathrm{T}}(t)\zeta(t)]\mathrm{d}t\}.$$

For zero initial condition, we can get

$$E\{\|\hat{y}(t)\|_2\} < \gamma E\{\|\omega(t)\|_2\} + \|\zeta(t)\|_2\}.$$

In addition, when $\omega(t)=0$ and $\zeta(t)=0$, we get the following inequality.

$$E\{\dot{V}(t)\} \leqslant -E\{\hat{y}^{\mathrm{T}}(t)\hat{y}(t) < 0 \tag{15}$$

Then there is a positive scalar $\varepsilon > 0$ to make the following inequality true.

$$E\{\dot{V}(t)\} \leqslant -\varepsilon E\{\|\xi(t)\|^2\} \leqslant -\varepsilon E\{\|\hat{x}(t)\|^2\} \tag{16}$$

For $\omega(t) \neq 0$ and $\zeta(t) \neq 0$, we prove that the closed-loop systems (10) under zero initial conditions has H_∞ stable performance.

Since the nonlinear coupling term XL is included in Theorem 3.1, the observer gain L cannot be directly calculated. Therefore, the following theorem provides a method to determine the observer gain matrix L. We define $Y=XL$, so $L=X^{-1}Y$. After linearization, we can get the following theorem.

Theorem 3.2 For a given level of disturbance rejection $\gamma > 0$, scalar $\alpha_0 \geqslant 0$, the closed-loop system (10) can be asymptotically stable, and meet the H_∞ performance, if there exist appropriate dimensions of positive definite matrices Q_1, Q_2, W_1, W_2, L, Y, symmetric positive definite matrix X and matrices U, N, $\bar{B}$ with appropriate dimensions to make the following inequality established.

$$\begin{bmatrix} \Gamma_{11} & \Gamma_{12} \\ \Gamma_{12}^{\mathrm{T}} & \Gamma_{22} \end{bmatrix} < 0 \tag{17}$$

$$\Theta_1 = \begin{bmatrix} Q_2 & U^{\mathrm{T}} \\ U & Q_2 \end{bmatrix} > 0,\ \Theta_2 = \begin{bmatrix} W_2 & N^{\mathrm{T}} \\ N & W_2 \end{bmatrix} > 0 \tag{18}$$

where

$$\hat{\Gamma}_{11} = \hat{\Gamma}_{111} - \hat{\Gamma}_{112} - \hat{\Gamma}_{113},$$

$$\hat{\Gamma}_{111} = \begin{bmatrix} \hat{Z}_1 & \hat{Z}_2 \\ \hat{Z}_2^{\mathrm{T}} & \hat{Z}_3 \end{bmatrix},$$

$$\hat{Z}_1 = \begin{bmatrix} \hat{\Sigma}_1 & \mathrm{XBK} & 0 & (1-\alpha_0)YC & 0 \\ * & \hat{\Sigma}_2 & 0 & 0 & 0 \\ * & * & 0 & 0 & 0 \\ * & * & * & \hat{\Sigma}_3 & 0 \\ * & * & * & * & 0 \end{bmatrix},$$

$$\hat{Z}_2 = \begin{bmatrix} 0 & -\mathrm{XBK} & 0 & \alpha_0 Y \\ 0 & \sigma\Phi & 0 & 0 \\ 0 & 0 & 0 & 0 \\ 0 & 0 & XF & -\alpha_0 Y \\ 0 & 0 & 0 & 0 \end{bmatrix},$$

$$\hat{Z}_3 = \begin{bmatrix} 0 & 0 & 0 & 0 \\ * & (\sigma-1)\Phi & 0 & 0 \\ * & * & -\gamma^2 I & 0 \\ * & * & * & -\gamma^2 I \end{bmatrix},$$

$$\hat{\Sigma}_1 = \mathrm{sym}\{XA\} + \{Q_1\},\ \hat{\Sigma}_2 = \sigma\Phi,$$

$$\hat{\Sigma}_3 = \mathrm{sym}\{XA\} - (1-\alpha_0)YC + W_1,$$

$$\hat{\Gamma}_{112} = \Pi_1^{\mathrm{T}}\Theta_1\Pi_1 + \Pi_2^{\mathrm{T}}\Theta_2\Pi_2 + Y_1^{\mathrm{T}}Y_1,$$

$$\Pi_1 = [e_1 - e_2 \quad e_2 - e_3]^{\mathrm{T}},$$

$$\Pi_2 = [e_4 - e_5 \quad e_5 - e_6]^{\mathrm{T}},$$

$$Y_1\} = [(1-\alpha_0)C \quad 0^{1\times 8}]^{\mathrm{T}},$$

$$\hat{\Gamma}_{113} = \Xi_1^{\mathrm{T}}\Xi_2^{-1}\Xi_1,$$

$$\Xi_1 = [\hat{\eta}Q_2H_\Delta \quad \hat{\eta}Q_2H_\Omega \quad \hat{\eta}W_2H_\varphi \quad \hat{\eta}W_2H_\psi],$$

$$\Xi_2 = \mathrm{diag}\{-Q_2, -Q_2, -W_2, -W_2\},$$

$$H_\varphi = [0^{1\times 3} \quad A - (1-\alpha_0)LC \quad 0^{1\times 3} \quad F],$$

$$H_\psi = [0^{1\times 3} \quad -LC \quad 0^{1\times 4} \quad L],$$

$$H_\Omega = [0^{1\times 3} \quad \bar{B}C \quad 0^{1\times 4} \quad -\bar{B}],$$

$$H_\Delta = [A \quad BK \quad 0 \quad (1-\alpha_0)\bar{B}C \quad 0 \quad 0 \quad -BK \quad 0 \quad \alpha_0],$$

$$\hat{\Gamma}_{12} = \begin{bmatrix} XB & 0 & 0 \\ 0^{2\times 1} & 0^{2\times 1} & 0^{2\times 1} \\ 0 & (1-\alpha_0)C^{\mathrm{T}}Y^{\mathrm{T}} & 0 \\ 0^{4\times 1} & 0^{4\times 1} & 0^{4\times 1} \\ 0 & 0 & \alpha_0 Y^{\mathrm{T}}, \end{bmatrix}$$

$$\hat{\Gamma}_{22} = \begin{bmatrix} -B^{\mathrm{T}}XB & 0 & 0 \\ * & -(1-\alpha_0)X & 0 \\ * & * & -\alpha_0 X \end{bmatrix}.$$

From the above theorems, we can get the event-triggered sliding mode LFC systems is asymptotically stable under H_∞ norm bound γ, and the observer gain is $L=X^{-1}Y$.

3.2 Accessibility analysis

In this section, we will further probe the accessibility of a given sliding surface $s(t)=0$. A set of sufficient conditions are given to ensure that the state trajectory of the closed loop system (10) enters the sliding domain near the specified sliding surface $s(t)=0$ in a finite time.

Theorem 3.3 For the closed-loop system (10), the sliding surface of form equation(7) is designed, and

the uncertain matrix X, L is obtained from the Theorem 3.2. Then, under the action of the following controller, the trajectory of the systems can reach the sliding surface in a finite time

$$u(t) = -\tau s(t) + K\hat{x}(t) - \delta(t) \cdot \mathrm{sgn}(s(t)) \quad (19)$$

where $\tau > 0$ is a constant, $\mathrm{sgn}(\cdot)$ is a symbolic function, $\delta(t)$ is expressed as

$$\delta(t) = \| (B^{\mathrm{T}}XB)^{-1} \| [\| B^{\mathrm{T}}XL\zeta(t) \| + 2 \| B^{\mathrm{T}}\mathrm{XLC}e(t) \|] \quad (20)$$

Proof The lyapunov function is designed as

$$V_s(t) = \frac{1}{2} s^{\mathrm{T}}(t)(B^{\mathrm{T}}XB)^{-1}s(t) \quad (21)$$

According to the formula (8), it can be obtained

$$\dot{s}(t) = B^{\mathrm{T}}XBu(t) - B^{\mathrm{T}}\mathrm{XBK}\hat{x}(t) + B^{\mathrm{T}}XL[(1-\alpha(t))Ce(t) + \alpha(t)\zeta(t)] \quad (22)$$

Substitute equation (19) into equation (22), then

$$\dot{s}(t) = B^{\mathrm{T}}XB[-\tau s(t) + K\hat{x}(t) - \delta(t) \cdot \mathrm{sgn}(s(t))] - B^{\mathrm{T}}\mathrm{XBK}\hat{x}(t) + B^{\mathrm{T}}XL[(1-\alpha(t))Ce(t) + \alpha(t)\zeta(t)] \leqslant B^{\mathrm{T}}XB[-\tau s(t) - \delta(t) \cdot \mathrm{sgn}(s(t))] + \| B^{\mathrm{T}}XL\zeta(t) \| + 2 \| B^{\mathrm{T}}\mathrm{XLC}e(t) \| \quad (23)$$

Then substitute equation (23) into equation (21), we have

$$\dot{V}_s(t) = s^{\mathrm{T}}(t)(B^{\mathrm{T}}XB)^{-1}\dot{s}(t) \leqslant -\tau \| s(t) \|^2 - s^{\mathrm{T}}(t)\delta(t) \cdot \mathrm{sgn}(s(t)) + \| s(t) \| (B^{\mathrm{T}}XB)^{-1}(\| B^{\mathrm{T}}XL\zeta(t) \| + 2 \| B^{\mathrm{T}}\mathrm{XLC}e(t) \|) \leqslant -\tau \| s(t) \|^2.$$

Obviously, for $s(t) \neq 0$, it is proved by the inequality (24) that the state trajectory of system (10) can be forced onto the sliding surface $s(t) = 0$ in a finite time.

Remark 2 The controller (19) designed by us can make the movement trajectory of system (10) reach the sliding surface in a finite time, which has strong robustness against the disturbance and deception attacks.

4 The simulation case

In this section, to prove the effectiveness of the proposed event-triggered SMC scheme in a networked multi-area power system, an example of three-area power system is presented. Table 1 shows the parameters of the associated three-area interconnected power systems[7].

Table 1. Three-area power system parameters.

parameter	Di	M_i	$\hat{R}_i$	T_{chi}	T_{gi}	β_i
Area1	1	10	0.05	0.30s	0.37s	$\frac{2}{\hat{R}_1}+D_1$
Area2	1.5	12	0.05	0.17s	0.4s	$\frac{4}{\hat{R}_2}+D_2$
Area3	1.8	12	0.05	0.20s	0.35s	$\frac{3}{\hat{R}_3}+D_3$

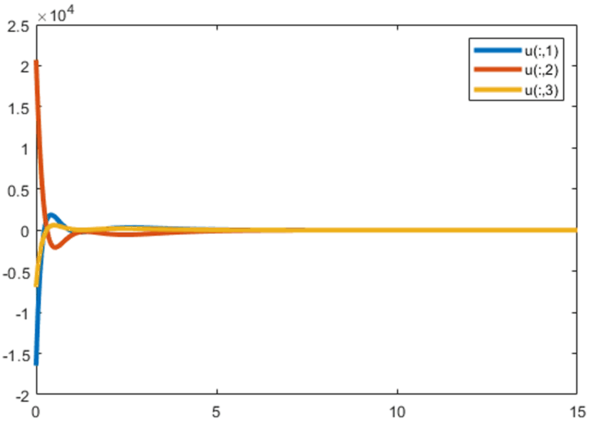

Figure 2. Control input trajectory of the three-area interconnected power system.

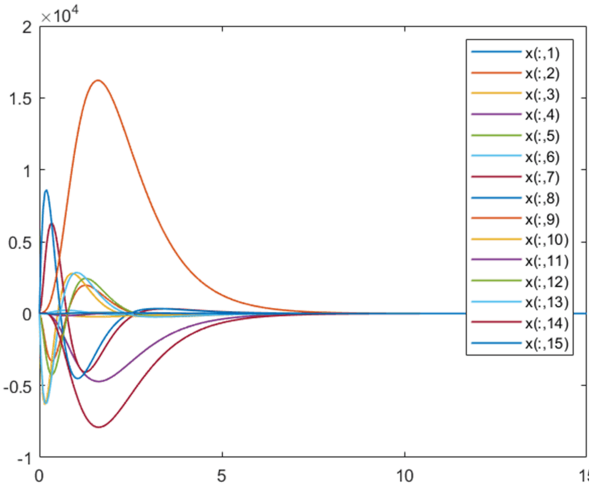

Figure 3. State trajectory of the three-area interconnected power system.

We can describe the systems parameter matrix as

$$A = \begin{bmatrix} A_{11} & A_{12} & A_{13} \\ A_{21} & A_{22} & A_{23} \\ A_{31} & A_{32} & A_{33} \end{bmatrix},$$

$$B = \mathrm{diag}\{B_1, B_2, B_3\},$$

$$C = \mathrm{diag}\{C_1, C_2, C_3\},\ F = \mathrm{diag}\{F_1, F_2, F_3\}.$$

Then the specific parameter matrix of each region can be obtained from Table 1, which will not be described here.

In our simulation, the synchronous power coefficient is set to $T_{12} = 0.2$ (pu/rad), $T_{13} = 0.12$ (pu/rad), $T_{23} = 0.25$ (pu/rad), the sampling period is set to $h = 0.01$ s, the rest of the parameter settings are $\alpha_0 = 0.2$, $\eta(t) = 0.1$. By solving the linear matrix inequality (17) in the Theorem 3.2, the coefficient matrix X and the observer gain $L = X^{-1}Y$ are obtained. According to the Theorem 3.3, the sliding mode controller is designed as equation (19). The simulation results are shown in Figures 2 to 6 below.

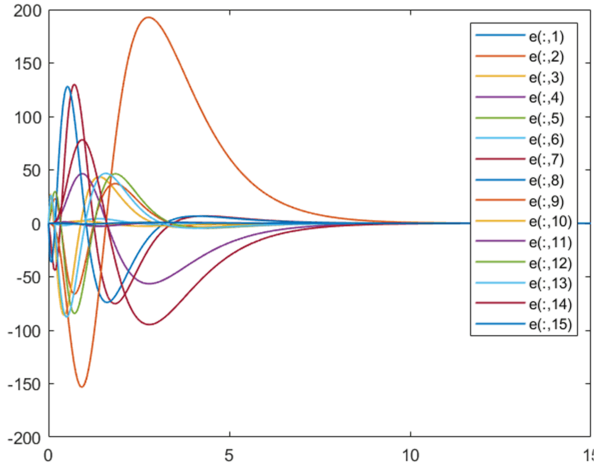

Figure 4. The observation trajectory of the three-area interconnected power system.

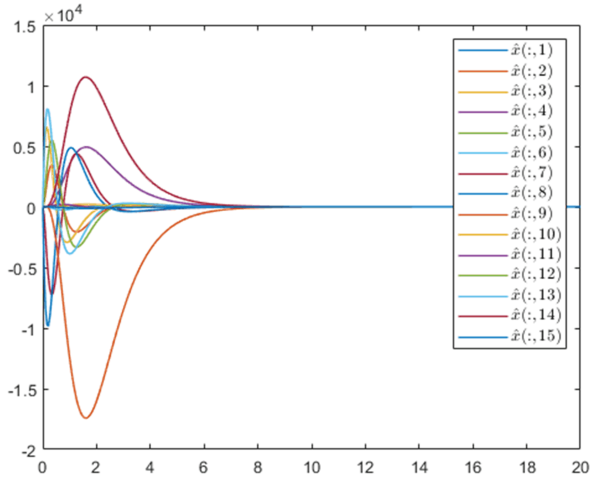

Figure 5. Error trajectories of the three-area interconnected power system.

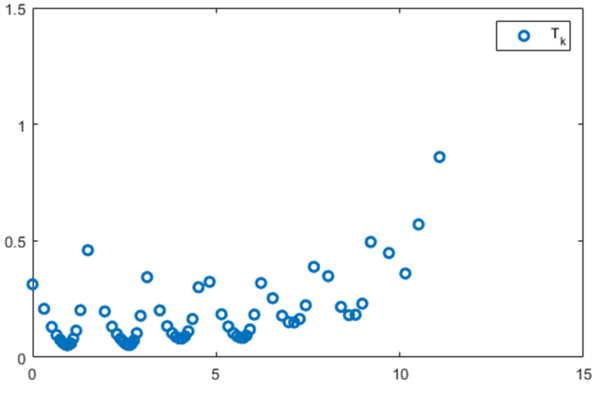

Figure 6. The trigger frequency under the event-triggered mechanism.

Figures 2 to 5 show the control input trajectory, state trajectory, state observation trajectory, and systems error trajectory of the three-area interconnected power systems. It can be clearly seen from Figures 3 and 4 that $x(t)$ and $\hat{x}(t)$ achieve asymptotical stability within 8 seconds under the action of the designed sliding mode controller (19). It indicates that our proposed event-triggered sliding mode LFC strategy can make the systems ultimately stable under the deception attacks. Figure 5 shows the error trajectory of the three-area interconnected power systems. It can be seen that the error trajectory of the systems tends to 0 within 10 seconds, which proves that the Luenberger observer (5) designed by us can accurately observe the actual value. The trigger frequency under the event-triggered mechanism is shown in Figure 6. It can be seen that not all the sampled data should be transmitted to the controller. Therefore, the introduction of event-trigger can effectively reduce the controller update frequency and reduce the network load.

5 Conclusion

The sliding mode LFC problem of the multi-area power systems under deception attacks was studied in this paper. An appropriate integral sliding surface and a Lyapunov-Krasovskii functional with double integrals have been constructed. Sufficient conditions for the exponential mean square stability with H_∞ performance have been derived by combining the characteristics of the LFC multi-area power systems and the event-triggered mechanism under deception attacks. Then the sliding mode controller has indicated that the trajectory of the closed-loop dynamic system can be driven to the specified sliding surface. Numerical simulated results have shown the applicability and effectiveness of the control scheme.

Acknowledgments

This work was supported in part by the National Natural Science Foundation of China (61903296, 61903353, U2003110), and in part by the Special Fund for Basic Scientific Research of the Central Universities (WK2100000013).

Conflict of interest

The authors declare no conflict of interest.

Author information

LIU Xinghua (Corresponding Author) is a professor with the Department of Power Grid Information and Control Engineering, School of Electrical Engineering, Xi'an University of Technology, Xi'an, China. He received the PhD degree in Automation from University of Science and Technology of China, Hefei, in 2014. From 2014 to 2015, he was invited as a visiting fellow at RMIT University in Melbourne. From 2015 to 2018, he was a Research Fellow with

the School of Electrical and Electronic Engineering, Nanyang Technological University, Singapore. His research focuses on state estimation and control of power systems, intelligent systems, autonomous vehicles, cyber-physical systems, robotic systems, etc.

BAI Dandan is a graduate student with the Department of Power Grid Information and Control Engineering, School of Electrical Engineering, Xi'an University of Technology, Xi'an, China. She received the BA. degree in Electrical Engineering and Automation from Yulin University, in 2019. Her research focuses on load frequency control.

SUN Baoren is currently the chief engineer of the production department of Huaneng Chaohu Power Generation Co. LTD, and is responsible for the operation and maintenance technology management and production technology tackling of the boiler, fuel, ash removal, desulfurization, denitration and other specialties of the power production system.

WEN Jiayan is currently an associate professor with the College of Electrical and Information Engineering, Guangxi University of Science and Technology, Liuzhou, China. He received the B. S. degree in automation from Guangxi University of Science and Technology, Liuzhou, China, in 2005, the M. S. degree in electrical machinery and apparatus from Hefei University of Technology, Hefei, China, in 2012 and the PhD degree in general mechanics and foundation of mechanics from Peking University, Beijing, China, in 2019. His research interests include multi-agent system, formation control, event-triggered control, autonomous vehicles, and cyber-physical systems.

LV Wenjun received the PhD degree in control science and engineering from the University of Science and Technology of China (USTC), Hefei, China, in 2018. He is currently an Associate Research Fellow with the School of Information Science and Technology, USTC. His research interests include robotics, interpretable machine learning and their applications in exploration geophysics.

LI Kun received the PhD degree in control science and engineering from the University of Science and Technology of China (USTC), Hefei, China, in 2018. He is currently an Associate Research Fellow with Institute of Advanced Technology, USTC. His research interests include nonlinear control theory and its application, robot trajectory and attitude control, artificial intelligence theory and its application in industry.

References

[1] Anderson P M, Fouad A A, Happ H H. Power system control and stability. IEEE Power Engineering Review, 2002, 15(2): 40.

[2] Kumar P, Kothari D P. Recent philosophies of automatic generation control strategies in power systems. IEEE Transactions on Power Systems, 2005, 20(1): 346-357.

[3] Kundur P. Power System Stability and Control. New York: McGraw-hill, 1994.

[4] Lu K, Zeng G, Luo X, et al. An adaptive resilient load frequency controller for smart grids with DoS attacks. IEEE Transactions on Vehicular Technology, 2020, 69(5): 4689-4699.

[5] Hu Z, Liu S, Luo W, et al. Resilient distributed fuzzy load frequency regulation for power systems under cross-layer random denial-of-service attacks. IEEE Transactions on Cybernetics, 2020, (99): 1-11.

[6] Tian E, Peng C. Memory-based event-triggering H1 load frequency control for power systems under deception attacks. IEEE Transactions on Cybernetics, 2020, 50(11): 4610-4618.

[7] Liu J, Gu Y, Zha L, et al. Event-triggered H1 load frequency control for multiarea power systems under hybrid cyber attacks. IEEE Transactions on Systems Man and Cybernetics: Systems, 2019, 49(8): 1665-1678.

[8] Peng C, Li J, Fei M. Resilient event-triggering load frequency control for multi-area power systems with energy-limited DoS attacks. IEEE Transactions on Power Systems, 2017, 32(5): 4110-4118.

[9] Chen C, Zhang K, Yuan K, et al. Novel detection scheme design considering cyber attacks on load frequency control. IEEE Transactions on Industrial Informatics, 2018, 14(5): 1932-1941.

[10] Bansal K, Mukhija P. Aperiodic sampled-data control of distributed networked control systems under stochastic cyberattacks. IEEE/CAA Journal of Automatica Sinica, 2020, 7(4): 1064-1073.

[11] Tripathy N S, Chamanbaz M, Bouffanais R. Robust stabilization of resource limited networked control systems under denial-of-service attack. 58th Conference on Decision and Control (CDC). Nice, France: IEEE, 2019: 7683-7689.

[12] Corradini M L, Cristofaro A. Robust detection and reconstruction of state and sensor attacks for cyber-physical systems using sliding modes. IET Control Theory & Applications, 2017, 11(11): 1756-1766.

[13] Huang X, Zhai D, Dong J. Adaptive integral sliding-mode control strategy of data-driven cyber-physical systems against a class of actuator attacks. IET Control Theory & Applications, 2017, 12(10): 1440-1447.

[14] 唐文秀, 奚文龙, 李志鹏,等. 基于滑模变结构和高增益状态观测器的直流电机位置控制. 中国科学技术大学学报, 2018, 48(1):82-88.
Tang W X, Xi H S, Li Z P, et al. Position control of DC-motor based on sliding mode variable structure and high-gain observer. J. Uiv. Sci. Tech. China, 2018, 48(1): 82-88.

[15] 康宇, 奚宏生, 季海波,等. 不确定多变量线性系统的快速收敛滑模变结构控制. 中国科学技术大学学报, 2003

(6): 91-98.
Kang Y, Xi H S, Ji H B, et al. Fast terminal sliding mode control of uncertain multivariable linear systems. J. Uiv. Sci. Tech. China, 2003, 33(6): 91-98.
[16] Jiang X, Mu X, Hu Z. Decentralized adaptive fuzzy tracking control for a class of nonlinear uncertain interconnected systems with multiple faults and DoS attack. IEEE Transactions on Fuzzy Systems, 2020, (99): 1-1.
[17] Yan S, Gu Z, Nguang S K, et al. Co-design of event-triggered scheme and H1 output control for Markov jump systems against deception attacks. IEEE Access, 2020, 8: 106554-106563.
[18] Liu X, Yu X, Ma G, et al. On sliding mode control for networked control systems with semi-Markovian switching and random sensor delays. Information Sciences, 2016, 337: 44-58.
[19] Peng C, Yue D, Han Q L. Communication and Control for Networked Complex Systems. Heidelberg: Springer, 2015.
[20] Park P, Ko J W, Jeong C. Reciprocally convex approach to stability of systems with time-varying delays. Automatica, 2011, 47(1): 235-238.

欺骗攻击下多区域互联电力系统的事件触发滑模负荷频率控制

刘兴华[1*],白丹丹[1],孙宝仁[2],文家燕[3],吕文君[4],李鲲[5]

1. 西安理工大学电气工程学院, 陕西西安 710054;
2. 华能巢湖发电有限责任公司, 安徽巢湖 238000;
3. 广西科技大学电气与信息工程学院, 广西柳州 545616;
4. 中国科学技术大学信息科学技术学院, 安徽合肥 230026;
5. 中国科学技术大学先进技术研究院, 安徽合肥 230088

摘要: 主要研究了多区域互联电力系统下遭受欺骗攻击的滑模负荷频率控制(load frequency control, LFC)问题. 在考虑欺骗攻击的情况下, 设计了一个龙伯格观测器来观测系统的状态, 利用 Lyapunov-Krasovskii (L-K)泛函法构造了一个积分滑模面, 并且给出了系统渐进稳定的充分条件. 然后, 基于观测器的滑模控制器将系统运动轨迹驱使到预先设计的滑模面上, 并使系统最终稳定. 在此基础上, 还引入了事件触发机制, 用以减少控制器更新和节点间通信的频率. 最后, 以一个三区域互联网络电力系统仿真验证了设计方案的有效性.

关键词: 负荷频率控制;欺骗攻击;滑模控制;事件触发机制